JOURNAL OF MATERIALS SCIENCE 16 (1981) 2218–2226

Influence of oxygen-rich inclusions on the $\gamma \rightarrow \alpha$ phase transformation in high-strength low-alloy (HSLA) steel weld metals

P. L. HARRISON, R. A. FARRAR
Department of Mechanical Engineering, The University of Southampton, Southampton, UK

Reducing the oxygen content of two submerged-arc, high-strength, low-alloy (HSLA) steel weld metals has been shown to depress $\gamma \rightarrow \alpha$ transformation temperatures and produce a marked change in the resultant microstructures. In weld metal of composition 0.12 wt % C, 1.35 wt % Mn, 0.29 wt % Si, 0.03 wt % Nb reducing the oxygen content from about 300 ppm to about 60 ppm decreased the transformation initiation temperature by about 30° C and changed the microstructure from acicular ferrite to parallel lath ferrite. In weld metal of composition 0.1 wt % C, 0.8 wt % Mn, 0.1 wt % Si, 0.01 wt % Nb reducing the oxygen content from about 600 ppm to about 300 ppm decreased the transformation initiation temperature by approximately 20° C and favoured the development of ferrite side-plates and acicular ferrite at the expense of the polygonal ferrite microstructure. In both weld metals the depressed transformation temperature is thought to be due to the larger γ-phase grain size developed when the volume fraction of small de-oxidation products is reduced. The marked microstructural change from fine-grained acicular ferrite to parallel lath ferrite which occurred when virtually all the de-oxidation products were removed suggests that these small de-oxidation products may also be of fundamental importance to the nucleation of acicular ferrite.

1. Introduction

In recent years the demand for high strength and good notch toughness in weld metals used for critical applications, such as off-shore structures and pipe-lines, has resulted in the development of welding consumables capable of depositing weld metals of very fine ferrite grain size. This fine-grained ferrite (typically with grain size 1 to 3 μm), known as acicular ferrite, provides increased strength via the Petch relationship and improved notch toughness due to its high-angle grain boundaries and high dislocation densities [1], which substantially impede the propagation of fast-running cleavage cracks.

Although the microstructure against mechanical properties relationships for acicular ferrite weld metals are now fairly well understood, there is as yet no clear indication of the exact mechanism of formation of this transformation product. Factors such as alloy hardenability, autenite grain size and weld cooling rate obviously play a very important role in determining whether or not acicular ferrite will form. However, recent investigations [2–4] have also suggested that the oxide inclusion distribution of the weld metal is of major importance.

Ito and Nakanishi [2] suggested that acicular ferrite (termed uniform fine-grained ferrite in the Japanese literature) was the dominant microstructural feature at oxygen contents above about 200 ppm. Below this level, lath-like structures were usually formed which were shown to have inferior resistance to crack propagation and therefore reduced weld-metal toughness. Abson *et al.* [3] confirmed this view by reducing the oxygen content of a submerged-arc weld metal from about 200 ppm to about 120 ppm using a laser remelting technique and observed a microstructural change

0022–2461/81/082218–09$02.90/0

from acicular ferrite to regions of thin parallel ferrite laths which they termed bainite. The model proposed to explain these observations suggested that acicular ferrite was nucleated directly on oxygen-rich inclusions of a certain type and size.

In contrast to these low oxygen-level studies, Cochrane and Kirkwood [4] have demonstrated that higher oxygen levels can also affect weld-metal transformation behaviour. By careful selection of welding consumables Cochrane and Kirkwood produced welds in which oxygen was the only major analytical variable, and found that the microstructure changed from fine acicular ferrite in the range 200 to 400 ppm to ferrite side-plates at levels above about 500 ppm. To explain these observations it was suggested that oxide-rich inclusions increased the nucleation rate of ferrite and in particular those inclusions associated with austenite grain boundaries favoured the development of ferrite side-plate structures.

Clearly, from the above studies, the phase-transformation behaviour of steel weld metals is complex and still far from fully understood and thus the present investigation was designed to seek to isolate the effect of oxygen inclusion-content. To achieve this, suitable submerged-arc high-strength, low-alloy (HSLA) steel weld metals were remelted under an argon atmosphere to reduce their oxygen contents. A high-speed dilatometer was then used to compare the $\gamma \rightarrow \alpha$ transformation temperature of the original weld metals and remelted samples under simulated welding conditions. Finally, optical metallography was carried out to characterize the various transformation structures produced.

2. Experimental procedure

2.1. Materials

The samples were selected from a series of submerged-arc weld metals produced with different flux/wire combinations on the same base-plates.

Sample E0 was produced using a commercial agglomerated basic flux (Oerlikon OP41TT) with SD3 wire. Sample E5 was produced using an experimental [5] agglomerated carbonate flux (503) also with SD3 wire.

Full details of the original welding conditions and consumable analyses are reported elsewhere [6] but it should be noted that the samples were taken from the columnar region of the top run of the weld bead deposit for dilatometric analysis and remelting.

Remelting was carried out in a non-consumable tungsten arc furnace keeping the charge molten for approximately 30 sec. Spectrographic (for metallic elements) and vacuum fusion (for gaseous elements) analyses were carried out before and after remelting.

2.2. Dilatometry

A Theta high speed dilatometer was used to monitor the weld metal $\gamma \rightarrow \alpha$ phase transformation during continuous cooling. Hollow cylindrical specimens, nominally of length 13 mm, outside diameter 5 mm and wall thickness 1 mm, were utilized. To ensure accurate temperature measurement, Pt–Pt10% Rh thermocopule wires (0.13 mm diameter) were welded to the outer surface of the specimens. To prevent oxidation or decarburization the dilatometer was vacuum purged (at a pressure of about 2×10^{-5} torr) and back-filled with high-purity argon.

The thermal cycle chosen for weld simulation consisted of austenization for 5 min at 1250° C followed by continuous cooling at a typical weld cooling rate of $13^{\circ}\,C\,sec^{-1}$ from 800 to 500° C [6]. During this cycle simultaneous recordings were made of temperature against time, dilatation against time, and dilatation against temperature behaviour.

2.3. Metallography and electron-probe microanalysis

After weld simulation, all dilatometer specimens were mounted, mechanically polished, and etched in 2% nital. Microstructural examinations and photomicrography were carried out using standard techniques.

To enable accurate assessment of austenite grain size the specimens were subsequently re-polished, broken out of their mounts, and re-subjected to the weld simulation thermal cycle under vacuum conditions (of approximately 10^{-4} torr). Quantitative metallography was carried out to determine the mean austenite grain sizes of these thermally-etched specimens.

Electron-probe microanalysis (EPMA) was performed to determine the chemical composition of the original de-oxidation products in Samples E0 and E5.

3. Results

3.1. Chemical analyses

The full spectrographic and vacuum fusion analyses for the weld metals and their remelts are given

TABLE I Chemical analyses of base-plate, weld metals and remelts (wt %)

Material	Specimen designation	Element																	
		C	Mn	Si	S	P	Nb	Ni	Cr	Mo	V	Ti	Al	Cu	B	Pb	Sn	Co	ppm O	ppm N
Base plate	E	0.15	1.34	0.39	0.035	0.028	0.061	0.08	0.07	< 0.01	< 0.01	< 0.01	0.006	0.23	< 0.001	< 0.01	0.02	0.01	304	156
Weld metal	E0	0.13	1.38	0.29	0.017	0.025	0.035	0.08	0.07	0.02	< 0.01	0.005	0.019	0.21	< 0.0005	0.01	0.01	0.02	305	91
Weld metal	E0 (remelted)	0.12	1.33	0.28	0.018	0.025	0.031	0.08	0.06	0.01	< 0.01	0.004	0.020	0.20	< 0.0005	ND	0.02	0.01	58	84
Weld metal	E5	0.10	0.80	0.10	0.021	0.019	0.008	0.15	0.06	0.02	< 0.01	0.006	0.006	0.19	< 0.0005	< 0.01	0.02	0.02	654	89
Weld metal	E5 (remelted)	0.10	0.85	0.11	0.024	0.021	0.011	0.15	0.06	0.02	< 0.01	0.008	0.007	0.19	< 0.0005	ND	0.02	0.02	278	94

ND = No data

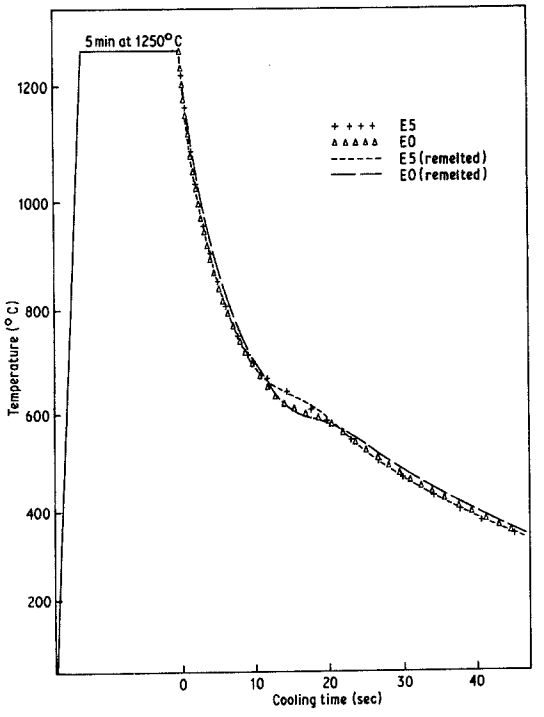

Figure 1 Thermal history of dilatometer specimens.

in Table I. It can be seen that remelting has successfully reduced weld-metal oxygen contents without significantly altering the balance of the other elements, especially those such as manganese and silicon, which are known to affect the hardenability of the weld metal.

3.2. Dilatometry

The thermal cycles of the original and remelted weld-metal dilatometer specimens are illustrated in Fig. 1. The cooling curves can be seen to be almost identical and their Newtonian character is typical of those obtained for actual welds [6]. It is interesting to note the partial thermal arrests in the cooling curves due to the $\gamma \rightarrow \alpha$ phase change. These thermal arrests show that the weld metals E5 and E5 (remelted) are transforming at higher temperatures than weld metals E0 and E0 (remelted), as would be expected from simple hardenability considerations.

The dilatometric results, presented as specimen dilatation against temperature curves, are shown in Figs 2 and 3. These curves confirm the above thermal arrest observations showing E5 and E5 (remelted) to transform at higher temperatures than E0 and E0 (remelted).

The point of major interest in Figs 2 and 3 is the effect of changing the oxygen content. In the

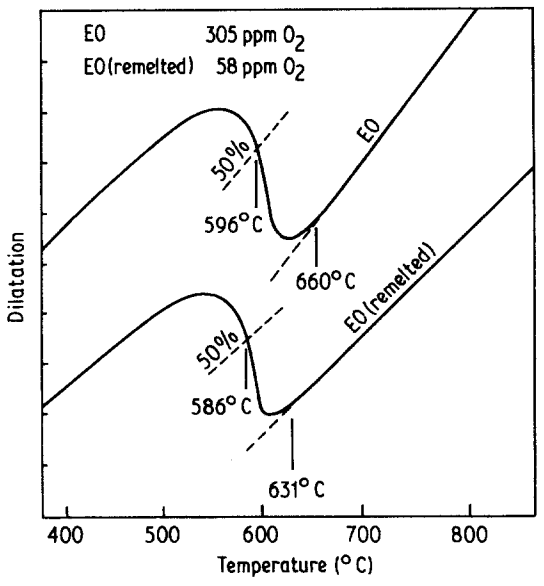

Figure 2 Dilatometric data for Specimens E0 and E0 (remelted).

case of weld metal E0, reducing the oxygen content from 305 ppm to 58 ppm can be seen to have reduced the transformation initiation temperature from 660° C to 631° C. Similarly, in the case of weld metal E5, reducing the oxygen content from 654 ppm to 278 ppm has reduced the transformation initiation temperature from 712° C to 693° C. A similar situation exists for the 50% transformation temperatures, also shown in Figs 2 and 3, although in this case the reduction in transformation temperature is less pronounced.

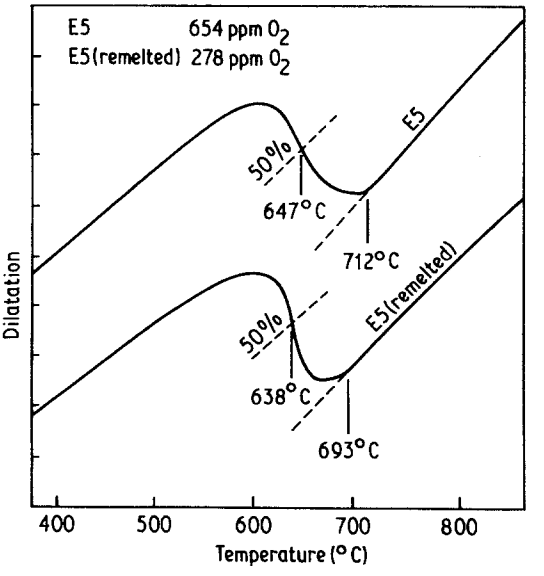

Figure 3 Dilatometric data for Specimens E5 and E5 (remelted).

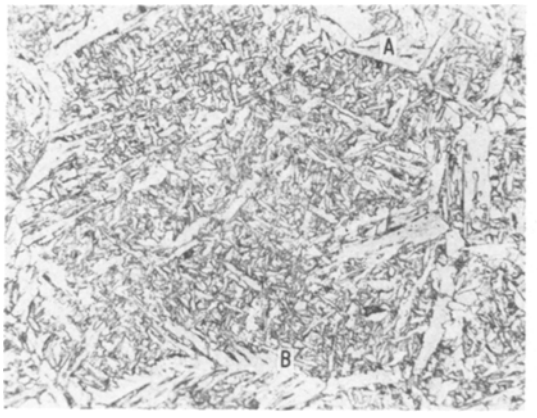

Figure 4 Microstructure of dilatometer Specimen E0; 2% nital etch, × 500 (A = grain-boundary ferrite allotriomorph, B = Widmanstätten ferrite side-plates).

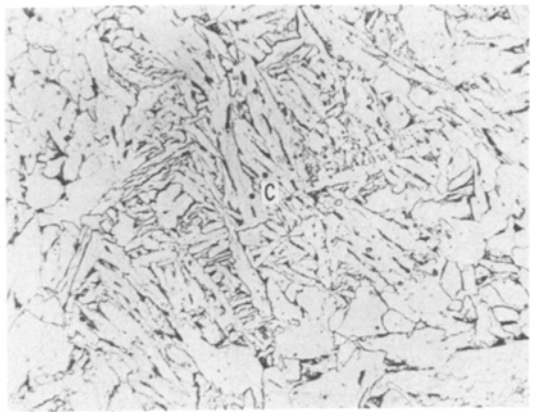

Figure 6 Microstructure of dilatometer Specimen E5; 2% nital etch, × 500 (C = deoxidation inclusions).

3.3. Metallography and electron-probe microanalysis

The results of the metallographic investigations are shown in Figs 4 to 7. The microstructure of dilatometer Specimen E0, shown in Fig. 4, is very similar to the original as-deposited microstructure which contained approximately 90% acicular ferrite, 7% polygonal ferrite and 3% ferrite side-plates. The microstructure can be seen to consist mainly of fine-grained acicular ferrite with bands of grain-boundary ferrite allotriomorphs delineating the prior austenite grain boundaries, (for example at A in Fig. 4). A few small regions of Widmanstätten secondary side-plates associated with some of the grain boundary allotriomorphs are also visible (for example, at B in Fig. 4).

The microstructure of dilatometer Specimen E0 (remelted) is shown in Fig. 5. It can be seen that a substantial change has occurred in the ferrite morphology. The predominant features are now regions, which consist of bundles of parallel ferrite laths, similar to those described by Ito [2] and Abson [3].

The microstructure of the lower hardenability weld metal dilatometer Specimen E5 is shown in Fig. 6. This microstructure again very closely resembles the original as-deposited microstructure which contained approximately 35% polygonal ferrite, 55% ferrite side-plates, 10% coarse acicular ferrite and a trace of pearlite. The higher oxygen content of this weld metal is apparent in the large number of spherical de-oxidation products observed (for example, at C in Fig. 6).

The microstructure of dilatometer Specimen E5 (remelted) is shown in Fig. 7. Again the familiar features of polygonal ferrite, ferrite side-plates, acicular ferrite and pearlite are present. However,

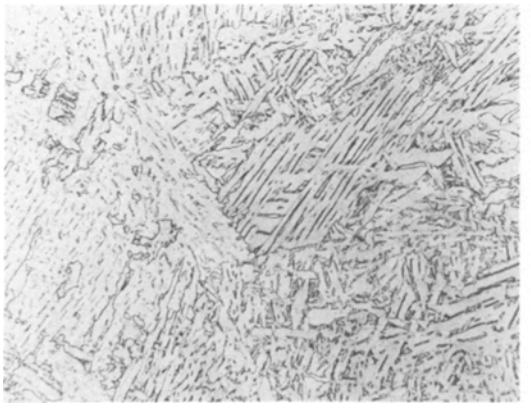

Figure 5 Microstructure of dilatometer Specimen E0 (remelted); 2% nital etch, × 500.

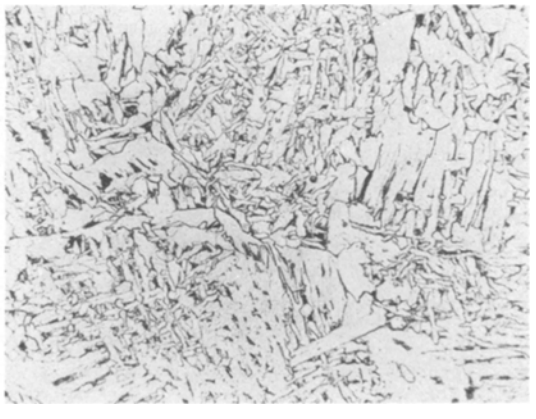

Figure 7 Microstructure of dilatometer Specimen E5 (remelted); 2% nital etch, × 500.

TABLE II Austenite grain-size determinations

Specimen	Mean ASTM number	Average linear intercept (μm)
E0	5.3	49
E0 (remelted)	4.3	72
E5	6.3	34
E5 (remelted)	4.0	78

the proportion of polygonal ferrite is significantly less than in Specimen E5 and the amounts of side-plate and coarse acicular ferrite structures have increased.

The results of the austenite grain-size determination are given in Table II. It should be noted that the reduction in oxygen content has resulted in larger austenite grain size in both weld metals. Figs 8 and 9 illustrate this effect showing micrographs of thermally-etched Specimens E0 and E0 (remelted). A number of surface oxides are also apparent which are believed to have formed during the thermal etching cycle.

The results of the quantitative EPMA inclusion analyses, corrected for absorption, atomic number and fluorescence, are shown in Table III. The results suggest the inclusion type in weld metal E0 is an aluminium manganese silicate-type containing small, but measurable, amounts of Ti, Nb, Ca and S, for example, Al_2O_3 : Mn(Fe)O : SiO_2.

The inclusion type produced by the 503 carbonate flux is thought to be an iron-rich manganese silicate containing measurable amounts of Al, Ti, Nb, Ca and S, for example, 2(Mn, Fe)O : SiO_2.

This latter type is thought to be typical of the types produced in welding situations where incomplete de-oxidation has occurred.

TABLE III Inclusion chemistry determined by EPMA

Element	Inclusion content (wt %)	
	Specimen E0	Specimen E5
Al	18.85	2.84
Fe	1.90	31.64
Ti	1.47	1.06
Mn	22.91	20.94
Nb	0.12	0.23
Si	10.88	13.06
Ca	0.43	0.15
S	0.34	0.80
O	43.08	29.29

4. Discussion

Taking the results obtained for the lower hardenability/high oxygen content weld metal, Specimen E5 (Fig. 3), it can be seen that reducing the oxygen content by about half reduces the $\gamma \rightarrow \alpha$ transformation start temperature by almost 20° C. From the microstructural observations of Figs 6 and 7 it can be seen that this reduction in transformation temperature has resulted in a reduction in the amount of the high-temperature polygonal ferrite being formed and an increase in the amount of lower temperature morphologies (ferrite side-plates and acicular ferrite) being formed. Comparing the prior austenite grain sizes of specimens E5 and E5 (remelted) it can be seen that the partial removal of oxygen-rich inclusions has enabled a larger austenite grain size to be developed in Specimen E5 (remelted) during the austenitizing cycle and thus grain growth has depressed the $\gamma \rightarrow \alpha$ transformation temperature. The magnitude of the effect is in good agreement with other recent studies on the effect of austenite

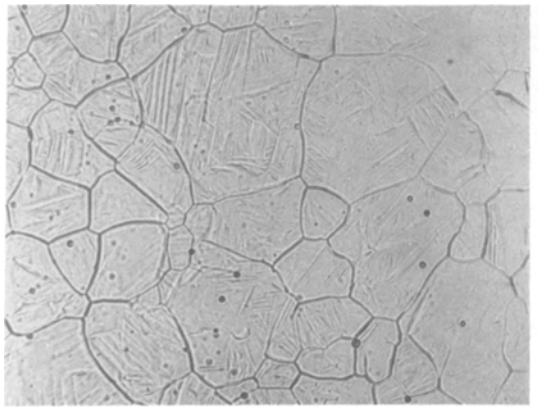

Figure 8 Austenite grain structure of dilatometer Specimen E0; thermal etch, × 200.

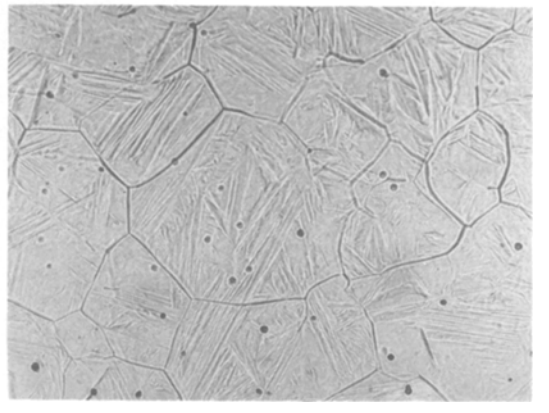

Figure 9 Austenite grain structure of dilatometer Specimen E0 (remelted); thermal etch, × 200.

TABLE IV Key to the notation used in Fig. 10

Notation	Explanation
PF	Polygonal ferrite: polygonal or equiaxed at slow cooling rates with grain-boundary allotriomorphs at faster cooling rates.
P	Pearlite: pearlite or pearlitic carbides.
FSP	Ferrite side-plates: side-plate structures growing directly from polygonal ferrite or grain boundary allotriomorphs, i.e., Widmanstätten secondary side-plates.
AF	Acicular ferrite: intragranular product of fine interlocking ferrite grains separated by high-angle boundaries; aspect ratios from about 3 : 1 to 10 : 1.
CAF	Coarse acicular ferrite: intragranular product formed at slower cooling rates than acicular ferrite with larger grain size and may be associated with carbides.
LF	Lath ferrite: intragranular product resembling bainite which sometimes forms amongst acicular ferrite or side-plate structures.
M	Martensite: low carbon content lath martensite.

grain size on transformation temperature in manual metal-arc C–Mn weld metals of similar composition [7].

The results for the higher hardenability/intermediate oxygen weld metal, Specimen E0 (Fig. 2), show that almost complete removal of oxygen also depresses the transformation initiation temperature, this time by almost 30° C. Again comparison of the prior austenite grain sizes (Specimens E0 and E0, remelted) reveals that increased grain size has resulted from the removal of the oxide-rich inclusions.

In both weld metals it is apparent that removal of oxide-rich inclusions reduces the pinning of austenite grain boundaries and allows larger austenite grains to become established. Owing to the change in the grain boundary area available, these larger grains subsequently transform at slightly lower temperatures during continuous cooling, and this explains the differences seen in the microstructures of Specimens E5 and E5 (remelted), see Figs 6 and 7.

Unfortunately the dramatic microstructural differences between Specimens E0 and E0 (remelted), Figs 4 and 5, is not so easily explained simply in terms of reduced transformation temperature. Considering the CCT diagram for weld metal E0 [8], Fig. 10 and Table IV, it is evident that a simple depression of the transformation temperature (due to rapid cooling in this case) promotes martensite rather than lath ferrite, in this weld metal, although a small proportion ($< 5\%$) of lath ferrite may be formed. The results of fully de-oxidizing a weld metal therefore, seems to produce a fundamental change in transformation behaviour, leading to the formation of parallel lath ferrite or classical "bainite"-like structures rather than acicular ferrite.

Previous investigators [2, 3, 9] have attempted to explain this change in transformation behaviour in terms of the availability of suitable nucleation sites for ferrite. Abson *et al.* [3] proposed that ferrite was nucleated by oxide inclusions. Ito and Nakanishi [2], on the other hand, suggested that TiN particles were the nucleation sites for acicular ferrite but noticed that oxygen strongly reduced the hardenability of the weld metal. More recently North *et al.* [9] have also suggested that TiN and VN promote acicular ferrite by providing suitable nucleation sites. They also noted that due to the rapid cooling of a weld metal the nitrides themselves may be nucleated on existing oxide inclusions. In this respect the oxygen content (oxide inclusion level) would still be an important factor in nucleating acicular ferrite.

Although there is little doubt that TiN and VN do help to promote acicular ferrite structures the very low levels of Ti and V in Specimen E0 probably rule out this mechanism. Another possibility is that ferrite nucleation occurs not directly on the inclusion substrate but rather on dislocations in the immediate vicinity of the inclusions. It is well established that the differential contraction between a hard inclusion and a softer matrix, brought about by rapid cooling, can produce strain fields within the matrix [10, 11]. The dislocations produced in this manner not only have the normal advantages as nucleation sites, i.e. that they aid formation of an incoherent interface between the new phase and the matrix and they promote diffusion and the relief of transformation stresses, but also this region of matrix close to the inclusion may be depleted in alloying elements such as Mn making nucleation in this region energetically more favourable.

To summarize, it would seem that reducing weld-metal oxygen-content (i.e. reducing the oxide inclusion-content) is responsible for an increased austenite grain size. This increased

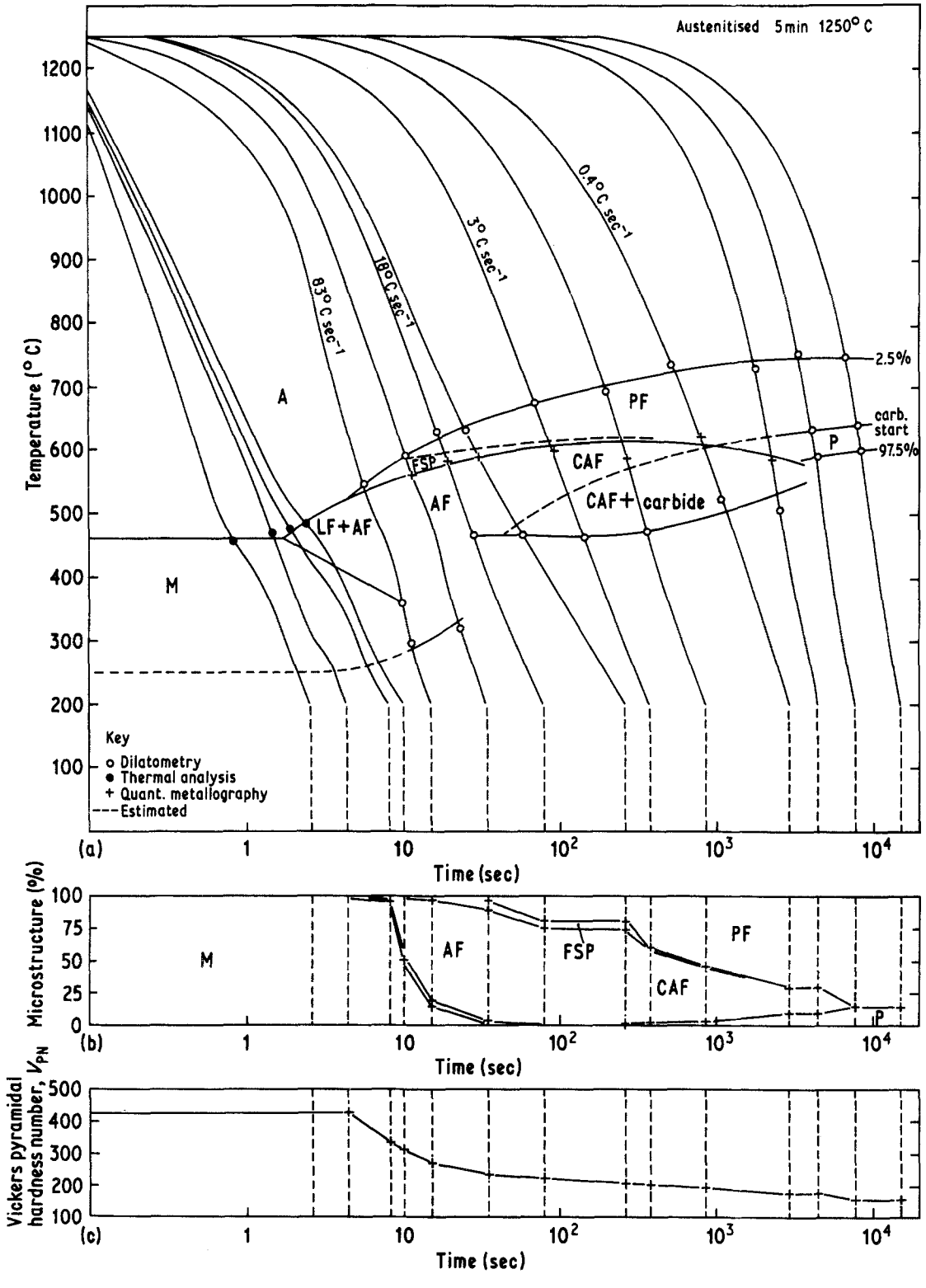

Figure 10 Continuous cooling transformation (CCT) diagram for weld Specimen E0, after Harrison [8]; see Table IV for key to notations used in the CCT diagram.

grain size depresses the $\gamma \rightarrow \alpha$ transformation temperature slightly which results in microstructures containing less polygonal ferrite but more ferrite side-plates or acicular ferrite. However, if almost all the oxygen is removed from the weld metal a fundamental change in transformation behaviour occurs resulting in structures more characteristic of those found in the heat affected zones of parent material of similar chemical compositions (in particular, similar oxygen content): i.e. bundles of parallel ferrite laths. This change in transformation behaviour is thought to be due to the almost complete removal of suitable nucleation sites for acicular ferrite, be they oxides, oxynitrides or the strain fields associated with the oxide-rich inclusions.

5. Conclusions

The results of this investigation suggest that oxygen content (i.e. the oxide inclusion level) is of fundamental importance to the behaviour of the $\gamma \rightarrow \alpha$ transformation in steel weld metals.

The effect of reducing the oxygen content of a low hardenability/high oxygen-content weld metal from 654 ppm to 278 ppm was to lower the transformation initiation temperature from 712 to 693° C. This resulted both in reduced polygonal ferrite and in increased proportions of ferrite side-plates and acicular ferrite.

Reducing the oxygen content of a higher hardenability/intermediate oxygen-content weld metal from 305 ppm to 58 ppm reduced the transformation initiation temperature from 660 to 631° C. In this case there was a dramatic change in microstructure from fine-grained acicular ferrite to a structure consisting of bundles of parallel ferrite laths.

In both weld metals the reduction in oxide inclusion-content resulted in development of a larger austenite grain structure, thus suggesting that these inclusions have a significant effect on grain-boundary pinning in weld metals.

It is concluded that the oxide rich inclusion contents of HSLA steel weld metals affect the $\gamma \rightarrow \alpha$ transformation, of reheated specimens, in two ways:

(a) Transformation temperature is altered due to the interaction of inclusions with austenite grain boundaries. Thus, higher inclusion contents tend to reduce austenite grain size and therefore favour higher temperature transformation products, e.g. polygonal ferrite and Widmanstätten secondary side-plates.

(b) Nucleation of fine intragranular ferrite (acicular ferrite) is aided by inclusions when factors such as austenite grain size, alloy hardenability and weld cooling rate combine to produce favourable conditions within the prior austenite grains.

Acknowledgements

The authors wish to thank the Director of the Marchwood Engineering Laboratories, CEGB and Dr D. J. Abson of the Welding Institute for their technical support in making this investigation possible. Thanks are also due to the Science Research Council for financial assistance throughout this research programme.

References

1. L. G. TAYLOR and R. A. FARRAR, *Weld. Metal Fab.* **43** (1975) 305.
2. Y. ITO and M. NAKANISHI, *Sumi Search* **15** (1976) 42.
3. D. J. ABSON, R. E. DOLBY and P. H. M. HART, in Proceedings of the Conference on Trends in Steels and Consumables for Welding (Welding Institute, Abington, Cambridge, 1978).
4. R. C. COCHRANE and P. R. KIRKWOOD, in Proceedings of the Conference on Trends in Steels and and Consumables for Welding (Welding Institute, Abington, Cambridge, 1978).
5. S. S. TULIANI, PhD Thesis, Southampton University, 1973.
6. M. N. WATSON, PhD Thesis, Southampton University, 1980.
7. P. L. HARRISON, unpublished work.
8. *Idem,* Mechanical Engineering Report number ME 79/24, Southampton University, 1979.
9. T. H. NORTH, H. B. BELL, A. KOUKABI and I. CRAIG, *Weld. Res. Sup.* 58 (1979) pp. 343-s.
10. D. A. JONES and J. W. MITCHELL, *Phil. Mag.* **3** (1958) 1.
11. J. M. ARROWSMITH, PhD Thesis, Cambridge University, 1960.

Received 2 December 1980 and accepted 5 February 1981.